JOURNAL OF OPTOELECTRONICS AND ADVANCED MATERIALS, Vol. 11, No. 11, November 2009, p. 1618 - 1626

Photoluminescence and electrical conductivity of silicon containing multilayer structures of diamond like carbon

N. DWIVEDI, S. KUMAR*, C. M. S. RAUTHAN, O. S. PANWAR, P. K. SIWACH
Plasma Processed Materials Group, National Physical Laboratory (CSIR),
K.S. Krishnan Road, New Delhi - 110 012. India

Photoluminescence and electrical conductivity of silicon containing multilayer structures of diamond like carbon were studied. These multilayer structures were deposited in a sequence a-Si:H/ Si-(a-C:H)/ a-C:H using conventional RF-PECVD technique. It was found that with the variation of silane partial pressure during the growth of middle layer (Si-(a-C:H)), the optical, electrical and photoluminescence properties of these multilayer structure varied. Electrical conductivity showed negative thermally activated process in these multilayer structure which disappeared after annealing the samples at 250 ^{0}C. The role of a-C:H as protective layer for luminescent Si-(a-C:H) layer has also been emphasized.

(Received November 3, 2009; accepted November 12, 2009)

Keywords: Multilayer structures, Diamond like carbon, Photoluminescence, Electrical conductivity

1. Introduction

Multilayer structures are of considerable interest to researchers due to its various tunable properties. Multilayer structures involving two most widely studied amorphous materials such as hydrogenated amorphous carbon (a-C:H) and hydrogenated amorphous silicon (a-Si:H) are quite interesting. These two materials have versatile applications. Hard a-C:H is also called diamond like carbon (DLC) due its strong mechanical and tribological properties such as high hardness, low friction and high wear resistance. All these lead to its industrial and space applications like hard coating for tools, wear resistance coating for computer hard disk and antireflection coating for space craft [1-5]. Similarly a-Si:H find wide applications in micro electronics and optoelectronics area, particularly in Thin film transistors (TFT's) and photovoltaic [6-7]. For last few years, a-C:H has also attracted considerable interest to researchers for possible use in other areas like photonic and optoelectronic applications/devices due to its tunable electrical, optical and luminescence properties. The electrical and luminescence properties of a-C:H can be tailored by band gap engineering, because its band gap can be tuned by varying π-π* bonding which is associated with sp^2 fraction of carbon [8].

In spite of all these unique properties, a-C:H have some drawbacks like poor adhesion particularly to non carbide forming substrates and high stress [9-10]. Thus, in order to modify and improve the a-C:H properties, and to overcome from its drawbacks, various incorporation of newer materials which are generally similar in structure to a-C:H like silicon (Si), nitrogen (N_2), metals (Ti, Cr, Cu) etc. have been used. Incorporation of these newer materials in a-C:H improves not only its mechanical and tribological properties but also improves its electrical, optical and luminescence properties and resolve simultaneously its stress and adhesion problems [4-11]. It is found that silicon incorporation in a-C:H is quite easier due to its similar tetrahedral bonding network [12] and beneficial in enhancing its mechanical and luminescence properties due to the enhancement of sp^3 fraction in its amorphous matrix [13]. In addition, Si incorporated a-C:H may be used in silicon-carbon based multilayer structures which may play a very important role in the improvement of the transport and luminescence properties due to presence of many layer boundaries in its structure. The RF plasma enhanced chemical vapor deposition (RF-PECVD) technique is a conventional way to grow multilayer structures just by choosing the process gas in the chamber as required for the deposition of several layer.

In this paper, the properties of silicon-carbon based multilayer structures consisting of three layer structures, namely a-Si:H bottom layer, Si-(a-C:H) middle layer and a-C:H as a top layer deposited by RF-PECVD technique have been reported. Each of these layers has its individual role in the improvement of the properties of whole structure. These multilayer structures were also characterized for stress, hardness, Fourier transform infrared spectroscopy (FTIR) and UV-visible transmission with main emphasis on photo luminescence and temperature dependent conductivity of silicon-carbon multilayer structure.

2. Experimental details

Amorphous Hydrogenated silicon–carbon multilayer structures were deposited using radio frequency (13.56 MHz) asymmetric capacitive coupled plasma enhanced chemical vapor deposition (RF- PECVD) technique on variety of substrates such as corning glass, micro slides, n-type single side polished silicon [100] wafers (resistivity 0.001-0.005 Ωcm and thickness 500-550 μm), p-type both side polished silicon [100] wafers (resistivity 3-6 Ωcm, thickness 500-550 μm). All the depositions were carried out without deliberate heating of the substrates. The silane (SiH_4) and acetylene (C_2H_2) were used as precursor gases. Substrates were cleaned by standard cleaning processes and treated in argon plasma in the process chamber at negative self bias of about 300 V to get rid of any contamination and moisture, prior to deposition. Four sets of samples were prepared and each of these sets involved three layer structures namely, bottom a-Si:H as an adhesive layer, middle Si-(a-C:H) as a bulk layer and top a-C:H as a surface or protective layer. During depositions, the gas pressures of silane 14 mTorr and acetylene 14 mTorr were adjusted with the help of needle valve for the bottom and top layer, respectively which were kept same for all the four sets, whereas for middle layer silane pressure was varied from 2 to 5 mTorr (silane partial pressure SPP = (SiH_4)/(SiH_4+Ar+C_2H_2) varied from 14-29 %) and the pressures of other two gases Ar and C_2H_2 were kept 5 mTorr and 7 mTorr, respectively. All depositions were performed at 50 mTorr and this pressure was achieved by adjusting the throttle valve after getting the desired pressure as mentioned earlier with the help of needle valve of respective gas as required to respective layer. All depositions were performed at self bias of 100 volts. The details of deposition parameters are given in Table 1. Thickness of middle layer Si-(a-C:H) was in the range of 730 nm-670 nm and bottom (a-Si:H) and top (a-C:H) layers were 20 nm and 150 nm, respectively.

Table 1. Process parameters for a-Si:H/Si-(a-C:H)/a-C:H multilayer structures growth.

Sample	Layer sequence	First layer SiH_4 Pressure (mTorr)	Second layer SiH_4+Ar+C_2H_2 (mTorr)	Third layer C_2H_2 pressure (mTorr)	Silane partial pressure for second layer [SiH_4/ SiH_4+Ar+C_2H_2]
Si-DLC 2	a-Si:H/Si-(a-C:H)/a-C:H	14	2+5+7 = 14	14	14 %
Si-DLC 3	a-Si:H/Si-(a-C:H)/a-C:H	14	3+5+7 = 15	14	20 %
Si-DLC 5	a-Si:H/Si-(a-C:H)/a-C:H	14	4+5+7 = 16	14	25 %
Si-DLC 6	a-Si:H/Si-(a-C:H)/a-C:H	14	5+5+7 = 17	14	29 %

Single layer a-C:H was also grown in order to estimate the properties of individual a-C:H layer used in these multilayer structures (a-Si:H /Si-(a-C:H) /a-C:H). Three sets of a-C:H films were grown at different acetylene gas (C_2H_2) pressure of 25 mTorr, 50 mTorr and 75 mTorr at constant negative self bias of 100 V where C_2H_2 pressure was adjusted initially at 14 mTorr and then throttled to 25 mTorr, 50mTorr and 75 mTorr for the three sets of a-C:H growth. Details of deposition for these a-C:H films have also been summarized in Table 2.

Table 2. Process parameters for the a-C:H growth.

Sample	Argon pressure (mTorr)	Acetylene pressure (m Torr)	Negative Self bias (V)
A	25	25	100
B	25	50	100
C	25	75	100

These multilayer structures have been characterized for photoluminescence (PL), conductivity as a function of temperature, UV-VIS transmission and FTIR. Thickness of these films was determined by stylus type instrument. The values of optical band gap of multilayer structures were determined by well known Tauc's plot of $(\alpha h\upsilon)^{1/2}$ versus hυ, where α is absorption coefficient and hυ is energy. The room temperature PL measurements were performed using Perkin Elmer LS 55 spectrometer. Dark conductivities were measured using Keithley electrometer 610C and Heico stabilized voltage power supply (model no. 1A501). Transmission was measured using UV-VIS 1601 spectrometer. FTIR measurements at room temperature were carried out using Perkin Elmer Spectrum Bx spectrometer in wave number range 400-4000 cm^{-1}. Single layer a-C:H films were also characterized using same characterization techniques, which were used for multilayer structures. The characterization of a-C:H layer seperately helps us to define the individual role of a-C:H and estimated the contribution of Si-(a-C:H) layer in over all properties of these multilayer structures. It is pointed out that thickness of a-Si:H layer is just 20 nm and it is speculated that it does not play any significant role in overall properties of multilayer stack except adhesion. After depositing these multilayer structures on glass, contacts were made by evaporating aluminum with 0.07 cm gap for coplanar in a vacuum of 10^{-6} Torr for electrical conductivity measurement.

3. Results and discussion

3.1. Stress & Hardness

Usually hard a-C:H (DLC) films are characterized for high hardness but stress in these films also increases with the increase in hardness. The incorporation of silicon in a-C:H reduces the stress without scarifying the hardness of the films. The variation of stress and hardness as a function of silane partial pressure for these multilayer structures were studied. Initially, stress in multilayer structures increases with the increase of silane partial pressure (SPP). The structures deposited at SPP of 14, 20 and 25 % exhibits the stress values 0.55, 0.95 and 1.1 GPa, respectively but beyond SPP of 25 %, stress start to decrease and found to be 1 GPa at 29 %. Similar behavior was also found with the hardness. Structures deposited at SPP of 14, 20 and 25 %, the hardness values were found to be 4.5, 5.0 and 12 GPa, respectively but beyond SPP of 25 %, hardness starts to decrease and becomes 7.5 GPa for the structure deposited at SPP of 29 %. The detailed studies of stress and hardness have been reported elsewhere with the figure of merit of stress per unit hardness found to be best for multilayer structures deposited at SPP of 25 % [14].

3.2. Transmission & FTIR

UV-VIS transmission of these silicon containing multilayer structures of DLC is shown in Fig. 1 and the values of E_g are estimated using Tauc's plot which are shown in the inset of Fig.1. The values of E_g varied from 1.33 to 1.46 eV for these multilayer structures deposited at various SPP's. The film deposited at SPP of 14 % exhibits the band gap 1.38 eV, which become lower of the order of 1.33 eV for the film deposited at SPP of 20 % and beyond SPP of 20 %, the E_g of the structures increased to 1.42 eV and 1.46 eV for the structures deposited at SPP of 25 and 29 %, respectively. Generally the E_g of value of a-Si:H lies between 1.7 to 1.9 eV as reported by various authors [15] where as E_g of a-C:H varies from 1 to 4 eV [16] depending upon deposition parameter. In the present case of multilayer structures, E_g values were found to be low as compared to pure a-Si:H and a-C:H. As E_g of a-C:H depends on π-π* bonding of sp^2 site. Initially Si incorporation in amorphous a-C:H matrix may be the cause for reduction in E_g of multilayer structures, because incorporation of silicon in a-C:H, reduce the π-π* gap of sp^2 site and hence reduce the band gap of the structures. Further, increase of Si (SPP beyond 20 %) increase the E_g, which may lead to onset of alloy formation (a-SiC:H). Lower E_g may also be attributed to defects associated with interfaces between various layers in these multilayer structures.

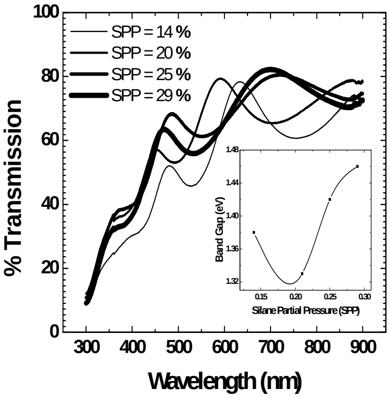

Fig. 1. Transmission spectra of multilayer structures grown at SPP of 14 %, 20 %, 25 % and 29 %. Inset show band gap variation as a function of silane partial pressure for multilayer structures.

FTIR spectra of as deposited silicon-carbon multilayer structures are shown in Fig. 2. The broad absorption band corresponding to Si-C bonding and weak absorption bands corresponding to C-C and C-H bonding confirm the incorporation of Si in a-C:H network. These films exhibit various stretching, wagging and olefinic vibration modes in different wave number regions. It is clear from Fig. 2 that the peaks found near 680-800 cm^{-1} region exhibit the bonding network between Si-CH_n whereas peaks at 780 and 990 exhibit Si-C stretching and SiC-H wagging vibration modes, respectively. Peak found at 1653 cm^{-1} represents the C-C stretching mode. The vibration peaks found near 2855 to 2960 cm^{-1} exhibit various CH bonding network. Peak at 2870 cm^{-1} shows sp^3CH_3 symmetric vibration mode where as its asymmetric mode occurs at 2960 cm^{-1}. Similarly sp^2CH_2 olefinic at 2950 cm^{-1}, sp^2CH_2

symmetric mode at 2855 cm^{-1}, sp^{3}CH$_2$ asymmetric at 2925 cm^{-1} and sp^{3}CH bond at 2915 cm^{-1} were obtained for these films.

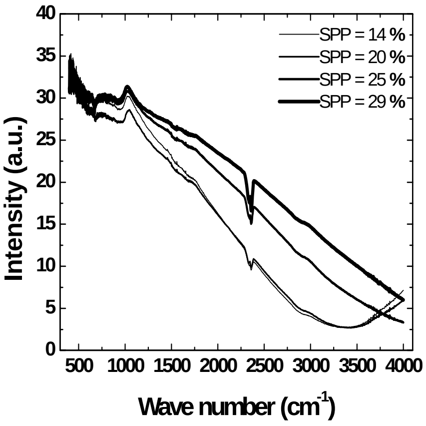

Fig. 2. FTIR spectra of as deposited silicon containing multilayer structures of a-C:H.

3.3. Photoluminescence (PL)

PL strongly depends on the defects present in the materials. These defects serve as recombination centers for charge carrier to recombine easily and exhibit efficient PL. a-Si:H and a-C:H both are very highly defective materials which contain very high defect density of the order of 10^{17}cm^{-3} and 10^{19}cm^{-3} as reported by various authors [17-18]. Both these materials exhibit very efficient PL spectra [19-20] but a-C:H is superior material for PL as compared to a-Si:H because a-C:H contain more defect density than a-Si:H which is very essential for quenching the PL [17-18]. PL may also quenched by paramagnetic Si dangling bonds which act as non radiative recombination centers [8]. PL study of multilayer structures involving these two highly defective materials is of significant interest.

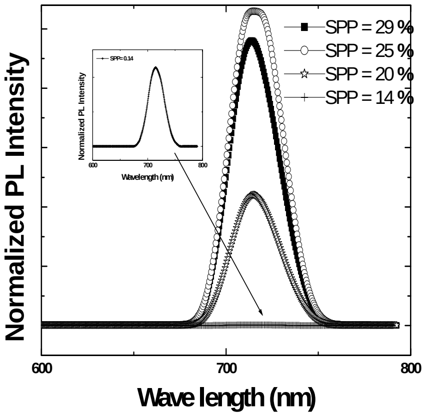

Fig. 3. PL spectra of silicon containing multilayer structures of DLC grown under varied SPP from 14 % to 29 %.

PL spectra of hydrogenated amorphous silicon - carbon multilayer structures are shown in Fig.3. It is evident from the figure that PL peaks are observed at about 714.5±0.5 nm. All these structures contain a-Si:H and a-C:H as a bottom and top layer, respectively which were grown under constant gas pressures of SiH$_4$ 14 mTorr and C$_2$H$_2$ 14 mTorr, whereas structure of middle layer Si-a-C:H was different due to the variation in Si content as SPP was varied. It is found that the variation in PL intensities in these films is governed by the variation in silane partial pressures in the middle layer. The film deposited under the SPP [SiH$_4$ / (SiH$_4$ + Ar + C$_2$H$_2$)] of 14 % for middle layer exhibits very low PL intensity. The intensity of PL peak is increased significantly on changing the silane partial pressure to 20 %.With further increase of SPP to 25 %, the PL intensity increases and becomes the highest of the four structures and beyond SPP of 25 % PL intensity starts decreasing and found to be comparatively lower at SPP of 29 % than SPP of 25 %. It is to be noted that stress per unit hardness of this particular structure is also better in comparison to the other structures. Since all these structures grown under same deposition condition contain a-C:H as a top layer, hence its contribution for PL efficiency will be the same for all the structures, whereas variable middle layer Si-(a-C:H), play very important role to influence the PL intensity. However, we may assume negligible contribution from a-Si:H layer for PL measurement because a-Si:H layer is very thin and situated in the bottom of the structure. PL property in a-C:H films can be explained by two phase model given by Robertson and O'Reilly [21]. PL property of a-C:H is governed by sp^2 site associated with π-π* weak bonding which segregate into clusters embedded in sp^3 bonded matrix. According to Robertson and Rusli et al.[22, 23], PL intensity in a-C:H is strongly dependent on sp^2 cluster size embedded in amorphous sp^3 a-C:H matrix and varies inversely proportional to its size. Therefore, when cluster size is large, PL intensity will be low and vice versa. Because in large cluster size, electron hole pairs generated by light become not so confined due to which it could not recombine easily, but on decreasing the sp^2 cluster size its PL intensity starts to increase due to quantum confinement of charge carrier. In the present case, silicon incorporation is found to influence the PL efficiency. Silicon exhibits tetrahedral sp^3 fraction. Si incorporation in a-C:H enhance the sp^3 fraction by reducing the size of sp^2 clusters. So on the basis of this, it may be clear that when there is change in SPP from 14 % to 21 %, Si incorporation in amorphous matrix of a-C:H enhance the sp^3 fraction by reducing the size of sp^2 clusters and hence electron-hole pairs in a cluster recombines radiatively and exhibits intense PL spectra. On further changing the SPP from 21 % to 25 %, the amount of Si incorporation in a-C:H increase, thus, sp^2 clusters become so small that the electron and holes recombine very easily to exhibit very efficient PL spectra. On further changing the SPP from 25 % to 29 %, the reduction in size of sp^2 clusters become saturated beyond which the PL intensity start to decrease. Thus, it seems that SPP of 25 % is the threshold pressure beyond which PL intensity starts to decrease. The cause of decrease in

PL intensity when SPP changes from 25 % to 29 % may be that after getting minimum size of sp^2 clusters as much as possible, Si incorporation does not influence the PL intensity. It is also clear from Fig.3, a very small shifting of peak was found in PL spectra of these multilayer structures. The structure deposited at SPP of 14 % exhibits the PL peak position at 714.5 nm which changes to 715 nm for the film deposited at SPP of 20 %. No change in PL peak (715 nm) was found for the structure deposited at 25 %. However, the structure deposited at SPP of 29 % shows PL peak at 714 nm. Since Si is very prone to oxidize in atmosphere, thus, in the present investigation to eliminate any chance of contribution of PL from Si-O layer, the top a-C:H layer has been used as protective layer to avoid this situation. Hence, it is emphasized that a-C:H is very useful protective layer for any luminescence device. PL peaks of all these multi layer structures were found near 715 nm region which exhibit red shift. Luminescence efficiency of these films also found to be good enough with narrow peaks. This type of outstanding PL results may lead to fabricate as a efficient display devices

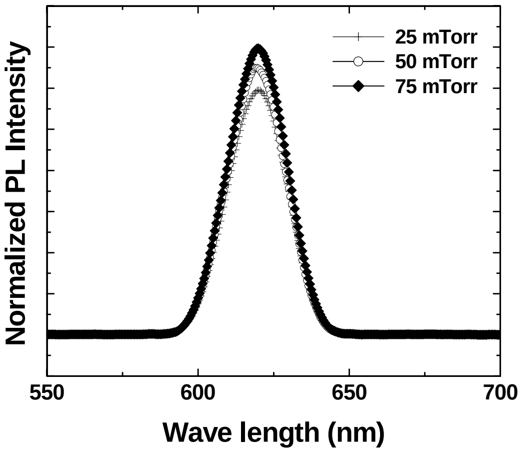

Fig. 4. PL spectra of single layer a-C:H films grown at C_2H_2 gas pressure 25, 50 and 75 mTorr.

In order to investigate the behavior of top a-C:H layer and importance of middle Si-(a-C:H)layer for PL intensity of multilayer structures, we have also grown single layer a-C:H films of same thicknesses under varied C_2H_2 gas pressure. The PL spectra of these as deposited a-C:H films are shown in Fig. 4. It is evident from the spectra that maximum PL intensity in these films remains constant and do not appear to change and are found to be 119.1, 129.8 and 139.4 a.u. at wave length 620, 619.5 and 620 nm, respectively. It is also noticeable that PL peak position for a-C:H films remains in the range 619.5 ± 0.5 nm and does not change. Whereas for multi layer structures, PL intensity varied significantly to the large values. Thus, an account of these considerations, it may be emphasized that middle Si-(a-C:H) layer is key factor to tune the PL intensity to the large value. On growing single a-C:H layer films, it become possible to discuss about the peaks position in multilayer films. Since peaks in single layer a-C:H films were found near 620 nm (orange shift) which changes to 715 nm (red shift) for multi layer structures. Reason for shifting the PL peaks from 620 to 715 nm may due to fact that PL peaks for pure a-Si:H films were obtained near 850-900 nm whereas for pure a-C:H it was near 600 nm as reported by various authors [24-25]. Since multilayer films contain both a-Si:H and a-C:H so the PL peaks obtained may be due to the combined contribution of both a-Si:H and a-C:H in the middle layer. At the moment it is unclear to us why there is no peak observed at 620 nm from the multilayer structures.

3.4. Dark Conductivity

Dark conductivity (σ_D) measurements performed on coplanar samples as a function of temperature for as deposited and annealed (at 250 ^{0}C for one hour) carbon-silicon multilayer structures are shown in Fig. 5 and Fig. 6 respectively. It is evident from these figures that as deposited samples shows anomalous behaviour of conductivity which were removed after annealing these samples. In the as deposited samples, initially σ_D increases with increasing the temperature. At a certain temperature called kink temperature T_1, σ_D becomes maximum beyond which it started decreasing. On further increasing the temperature, σ_D decreases, but once again at second kink temperature T_2 it gets its minimum value beyond which it starts increasing with increasing temperature. The magnitude of σ_D for these films depends on the SPP which is amount of Si present in a-C:H. The variation of σ_D is just one order with the change of temperature from room temperature (RT) to about 200 ^{0}C. The maximum value of σ_D for the structures deposited at SPP of 14 % and 21 % were found to be of the order of 3×10^{-8} $\Omega^{-1}cm^{-1}$ and 4×10^{-8} $\Omega^{-1}cm^{-1}$, respectively which changes to 8×10^{-8} $\Omega^{-1}cm^{-1}$ and 9×10^{-8} $\Omega^{-1}cm^{-1}$ for the structures deposited at SPP of 25 % and 29 %, respectively.

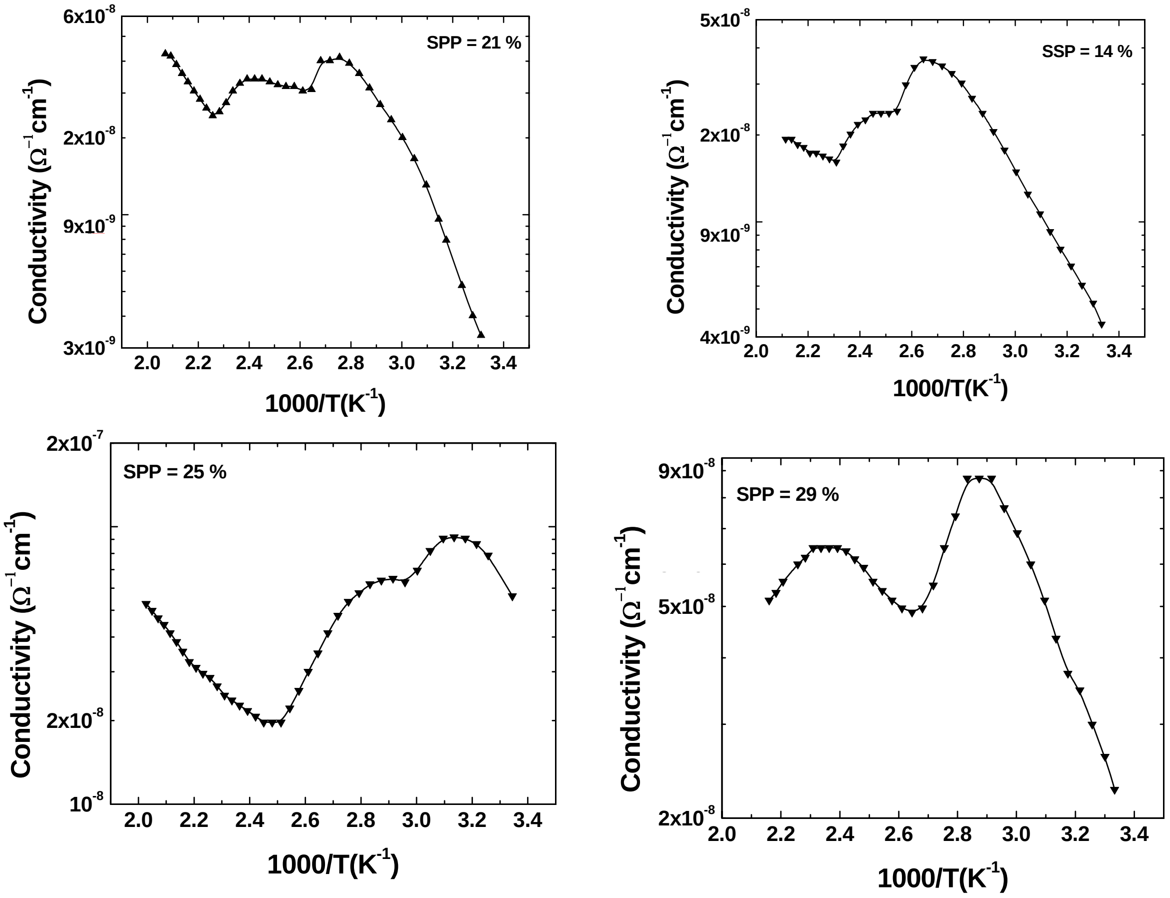

Fig.5. Temperature dependent conductivity of as deposited multilayer structures deposited at SPP of 14 %, 20 %, 25 % and 29 %.

Usually, conductivity increases with increase in the temperature. But in the present case of silicon-carbon multilayer structures, the observed behavior of conductivity deviates from their conventional behavior due to the fact that as a-Si:H is comparatively lesser thermally stable material than a-C:H, and during the conductivity measurement these structures are annealed due to variation in temperature[26-28].

The conductivity (σ_D) in disordered materials is generally governed by a thermally activated process, given by

$$\sigma_D = \sigma_0 \, e^{-\Delta E / kT}$$

where σ_0 is conductivity pre exponential factor, ΔE is activation energy, k is the Boltzmann's constant and T is the temperature in kelvin.

But in the present case we have observed multiple thermally activated processes; the resultant dark conductivity (σ_D) may be given by

$$\sigma_D = \sigma_{01} \, e^{-(\Delta E_1)/kT_1} + \sigma_{02} \, e^{-(-\Delta E_2)/kT_2}$$

where σ_{01} and σ_{02} are conductivities pre exponential factors, T_1 and T_2 are kink temperatures; ΔE_1 and ΔE_2 are the two activation energies which correspond to increase and decrease in conductivity behaviour, respectively. There is more than one process in thermally activated positive and negative activation regime as can be seen in Fig.5. Negative activation energy in the above expression may be seen as due to interfaces boundaries and different thermal coefficient (i.e heating gradient) of three layers from bottom to top. Other view in this regard may be due to contribution from Si-(a-C:H) layer. The similar behavior of conductivity is also observed by Baja et al. [26] and Vetter et al. [29] in carbon rich cathodic amorphous silicon carbon alloys and PECVD amorphous silicon carbon films, respectively. These authors have shown that this negative activation effect can be removed after annealing the sample [26, 29].

On increasing temperature above room temperature, bottom layer a-Si:H of multilayer films is first heated and covalent bond present in a-Si:H are broken, which leads to the formation of electron hole pairs. Therefore, initially on increasing the temperature, conductivity in these films are increased. On further increasing the temperature more covalent bonds are broken and conductivity is further increased, but beyond first kink temperature T_1, it is expected that middle layer also start contributing for conduction mechanism and consequently conductivity started decreasing with further increase of temperature. This kind of behavior of conductivity for these films are found due to lesser thermal stability of a-Si:H in comparison to a-C:H. Although deviation is not large enough because carbon is also present in Si-(a-C:H). With further increase in the temperature to larger value, top layer a-C:H also contribute for conduction mechanism and thus conductivity started increasing. Above second kink temperature T_2, when top layer started to contributing for the conductivity, the concentration of thermally stable a-C:H becomes more than that of a-Si:H.

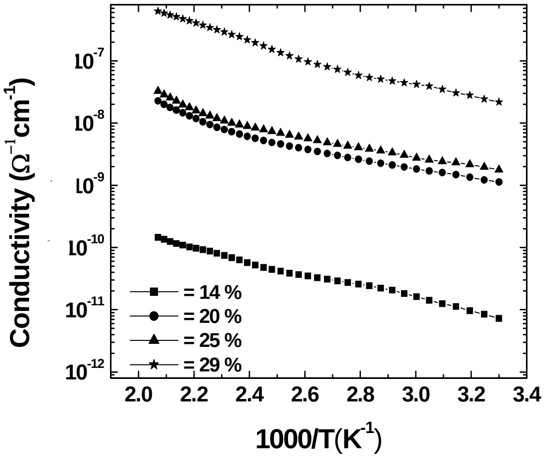

Fig. 6. Temperature dependent conductivity of multilayer structures annealed at 250 ^{0}C for one hour in a vacuum of the order of 10^{-6} Torr.

Fig. 6 shows the results of temperature dependent conductivity for multilayer structures annealed at 250 ^{0}C for one hour in a vacuum of the order of 10^{-6} Torr. It is evident from the figure that conductivity deviation in multilayer structures was reformed by the structural rearrangements and decrease in defects, caused by annealing at 250 ^{0}C. These annealed multilayer structures also exhibit two activation energy having kink temperature around 110±5 ^{0}C. The values of first activation energy (ΔE_1) evaluated for these films were found to be 0.20 eV, 0.15 eV, 0.14 eV and 0.17eV deposited at SPP 14 % , 20 %, 25 % and 29 %, respectively which are comparatively lower than the values of second activation energy ((ΔE_2) evaluated which are found to be 0.23 eV, 0.3 eV, 0.29 eV and 0.3 eV. One can also see from Figs. 5 and 6 that after annealing, conductivity magnitudes were significantly changed due to the structural rearrangements of the structures. The structure deposited at SPP of 14 % exhibits conductivity 7.26×10^{-12} Ω^{-1}cm^{-1} and 4.53×10^{-10} Ω^{-1}cm^{-1} at 30 ^{0}C and 210 ^{0}C, respectively which changes to 1.1×10^{-9} Ω^{-1}cm^{-1} and 2.27×10^{-8} Ω^{-1}cm^{-1} for film deposited at SPP of 20 %. However, the structure deposited at SPP of 25 % shows σ_D as 1.77×10^{-9} Ω^{-1} cm^{-1} and 3.26×10^{-8} Ω^{-1}cm^{-1} at above temperatures, respectively which changes to 2.18×10^{-8} Ω^{-1}cm^{-1} and 6.27×10^{-7} Ω^{-1}cm^{-1} for the film deposited at SPP of 29 %.

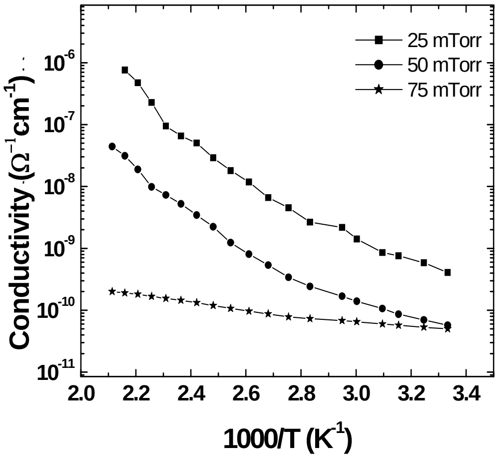

Fig. 7. Temperature dependent conductivity of single layer a-C:H film grown at C_2H_2 gas pressure 25, 50 and 75 mTorr.

Temperature dependent conductivity measurement were also carried out for some single layer a-C:H film deposited under varied acetylene gas pressures of 25, 50 and 75 mTorr. Conductivity in all these films obeys a conventional thermally activated process [30,31] without any negative activation behavior as observed in multilayer structure. Since films deposited at acetylene gas pressure 25 mTorr and 50 mTorr exhibits two thermally activated conduction processes hence resultant conductivity is given by

$$\sigma_D = \sigma_{01} e^{-(\Delta E_1)/kT_1} + \sigma_{02} e^{-(\Delta E_2)/kT_2}$$

The activation energy ΔE_1 is found to be dominant at lower temperature while ΔE_2 is found to be dominant at higher temperature beyond kink temperature. The kink temperature for these a-C:H films occur at around 60±6 ^{0}C. The values of ΔE_1 and ΔE_2 for the a-C:H film deposited at C_2H_2 pressure 25 mTorr were found to be 1.17 eV and 1.2 eV, respectively. Whereas it is 0.55 eV and 1.32 eV, respectively for film deposited at C_2H_2 pressure 50 mTorr.. However, film deposited at 75 mTorr exhibits single activation conduction process having activation energy of the order of 0.27 eV. Temperature dependent conductivity is strongly dependent on precursor gas pressure, which is decreased on increasing the precursor gas pressure. Thus, it is clear from the Fig. 7 that maximum value of conductivity was found for the film deposited 25 mTorr C_2H_2 gas pressure, which decreases to considerable large value for the film deposited at C_2H_2 pressures 50 mTorr and 75 mTorr, respectively. From conductivity data of a-C:H films, it is confirmed that conductivity deviation in multi layer films do not occur because of a-C:H. Further one should see conduction mechanism in a-Si:H, Si-(a-C:H) and a-C:H individually also . However, average conduction property of these layers in a sequence a-Si:H/Si-(a-C:H)/a-C:H is quite different (Fig.6)

In a-C:H, the four fold coordinated sp^3 site contain no free electrons because each carbon atom make proper bonding with their nearest neighbors carbon atoms, but three fold coordinated sp^2 site associated with π-π^* bonding contain one free electron. Thus transport property of amorphous carbon is governed by the localized π states over large energy range. The nature of density of states is very similar in a-Si:H to these in Si-(a-C:H) and hence the carrier conduction property in these disordered material is also expected to be similar to a-C:H [32].

4. Conclusions

Silicon containing multilayer structures of DLC grown by asymmetric capacitively coupled RF-PECVD technique have been characterized by means of stress, hardness, photoluminescence, conductivity, UV-VIS transmission and FTIR spectroscopy. Stress of the structures was reduced without affecting its hardness values. These multilayer structures exhibit very intense visible PL spectra. The PL intensity of the structures depends on amount of silicon which increases with increasing SPP from 14 % to 25 %. However, beyond SPP of 25 % , PL intensity starts decreasing. Negligible peak shifting (714.5±0.5 nm) was found for PL of these multilayer structures. Positive and negative activated conduction processes were observed during temperature dependent conductivity measurement for as deposited multilayer structures, which are resolved by annealing these samples at 250 ^{0}C for one hour. Band gap values of these structures deposited at SPP of 14 %, 20 %, 25 % and 29 % were found to be 1.38 eV, 1.33 eV, 1.42 eV and 1.46 eV, respectively. FTIR spectra exhibits various bonding between Si-C near 600-1000 cm^{-1} region which reveals the incorporation of Si in a-C:H. Several C-H stretching modes were also found near 2900 cm^{-1} with their usual characteristics of a-C:H. All these multilayer results are compared with those as deposited single layer a-C:H films in order to distinguish the individual role of Si-(a-C:H) in multilayer structures.

Acknowledgement

The authors are grateful to the Director, National Physical Laboratory, New Delhi (India) for his kind permission to publish this paper. The author wish to thank Dr. Harnath for PL measurement. We acknowledge CSIR, Govt. of India for sponsoring Network Project NWP-0027 and for their financial support.

References

[1] M. Silinnskas, A. Grigonis, Z. Rutkuniene, J. Maniks, V. Kulikauskas, Physics and Chemistry of Solid State **6**, 394 (2005).
[2] A. K. Gangopadhyay, P. A. Willermet, W. C. Vassell, M. A. Tamor, J. Tribology International **30**, 19 (1997).
[3] J. Robertson, Phys. Stat. Sol. (a) **205**, 2233 (2008).
[4] A. Grill, IBM Journal of Research and Development **43,** 147 (1999).
[5] Y. Tzeng, Diamond Films and Technology **1,** 31 (1991).
[6] D. Y. Park, K. H. Moon, S. Y. Choi, Mol. Cryst. **499,** 169 (2009).
[7] E. Klimovsky, A. Sturiale, F.A. Rubinelli, Thin Solid Films **515,** 4826 (2007).
[8] J. Robertson, Phys. Rev. B **53**, 16302 (1996).
[9] D. R. Mckenzie, D. Muller, B. A. Pailthorpe, Phys. Rev. Lett. **67**, 773 (1991).
[10] P. J. Fallon, V.S. Veerasami, C. A. Davis, J. Robertson, G. A. J. Amaratunga, W. I. Milne, J. Coskinen, Phys. Rev. B **48,** 4777 (1993).
[11] M. Ban, T. Hasegawa, Surf. and Coat. Technol. **162**, 1 (2003).
[12] F. Demichelis, G. Kaniadakis, A. Tagliaferro, E. Tresso, Phys. Rev. B **40**, 1247 (1989).
[13] S. E. Ong, S. Zhang, H. Du, D. Sun, Diamond and Related Materials 1**6,** 1628 (2007).
[14] S. Kumar, N. Goyal, P.N. Dixit, C.M.S. Rauthan, 51st SVC Annual Technical Conference Proceedings Chicago, p. 722 (2008).
[15] H. Matsuura, Jpn. J. Appl. Phys. **27**, L516 (1988).
[16] J. Robertson, Phys. Stat. Sol. (a) **186**, 177 (2001).
[17] C. Godet, Proceeding of the 1st international specialist meeting on Amorphous Carbon, p.186 (1997).
[18] J. D. Carey, S. R. P. Silva, Phys. Rev. B **70**, 235417 (2004).
[19] I. Umezu, T. Murota, M. Kawata, Y. Takashima, K. Yoshida, M. Inada, A. Sugimura, Jpn. J. Appl. Phys. **39,** L844 (2000).
[20] M. Koos, I. Pocsik, J. Erostyak, A. Buzadi, J. Non-Cryst. Solids **227-230**, 579 (1998).
[21] J. Robertson, E. P. O'Reilly, Phys. Rev. B **35**, 2946 (1987).
[22] Rusli, G. A. J. Amaratunga, S. R. P. Silva, Thin Solid films **270,** 160 (1995).
[23] J. Robertson, Adv. Phys. **35**, 317 (1986).
[24] P.K. Bhat, D.J. Dunstan, I.G. Austin, T.M. Searle, J. Non-Cryst. Solids **59-60,** 349 (1983).
[25] M. Pandey, D. S. Patil, Diamond and Related Materials **16**, 1912 (2007).
[26] A. L. B. Neto, F. Finger, S. S. Camargo Jr, Braz. J. Phys. **26**, 359 (1996).

[27] S. R. P. Silva, G. A. J. Amaratunga, C. N. Woodburn, M. E. Welland, S. Haq, Jpn. J. Appl. Phys. **33**, 6458 (1994).
[28] S. Bhattacharyya, S. R. P. Silva, Thin Solid Films **482**, 94 (2005).
[29] M. Vetter, C. Voz, R. Ferre, I. Martin, A. Orpella, J. Andreu, R. Alcubilla, Thin Solid Films **511-512,** 290 (2006).
[30] T. Sugino, J. Shirafuji, Phys. Stat. Sol. **154**, 371 (1996).
[31] A. Tibrewala, E. Peiner, R. Bandorf, S. Beihl, H. Luthje, J. Micromech. Microeng. **16**, S75 (2006).
[32] D. Dasgupta, F. Demichelis, C.F. Pirri, A. Tagliaferro, Phys. Rev. B **43**, 2131 (1991).

---

[*] Corresponding author: skumar@nplindia.org